

This is an Open Access document downloaded from ORCA, Cardiff University's institutional repository: <https://orca.cardiff.ac.uk/id/eprint/104568/>

This is the author's version of a work that was submitted to / accepted for publication.

Citation for final published version:

Pritchard, Manon , Jack, Alison, Powell, Lydia , Sadh, Hina, Hill, Katja E. , Thomas, David W. and Rye, Philip D 2017. Alginate Oligosaccharides modify hyphal infiltration of *Candida albicans* in an in vitro model of invasive Human Candidosis. *Journal of Applied Microbiology* 123 (3) , pp. 625-636. 10.1111/jam.13516

Publishers page: <https://doi.org/10.1111/jam.13516>

Please note:

Changes made as a result of publishing processes such as copy-editing, formatting and page numbers may not be reflected in this version. For the definitive version of this publication, please refer to the published source. You are advised to consult the publisher's version if you wish to cite this paper.

This version is being made available in accordance with publisher policies. See <http://orca.cf.ac.uk/policies.html> for usage policies. Copyright and moral rights for publications made available in ORCA are retained by the copyright holders.



1 Alginate Oligosaccharides Modify Hyphal Infiltration of *Candida albicans* in an *In Vitro* Model of
2 Invasive Human Candidosis

3

4 Abbreviated Running Headline: Altering *In Vitro* Hyphal Invasion

5

6 Manon F. Pritchard¹, Alison Jack¹, Lydia C. Powell¹, Hina Sath¹, Philip D. Rye², Katja E. Hill¹,
7 David W. Thomas¹.

8

9 ¹ Advanced Therapies Group, Cardiff University School of Dentistry, College of Biomedical and Life
10 Sciences, Cardiff, UK

11 ² AlgiPharma AS, Sandvika, Norway

12

13

14 **Correspondence**

15 Manon F. Pritchard, Advanced Therapies Group, Cardiff University School of Dentistry, College of
16 Biomedical and Life Sciences, Cardiff, CF14 4XY, UK

17 E-mail: pritchardmf@cardiff.ac.uk

18

19

20

21 **Abstract**

22 **Aims:** A novel alginate oligomer (OligoG CF-5/20) has been shown to potentiate antifungal therapy
23 against a range of fungal pathogens. The current study assessed the effect of this oligomer on *in vitro*
24 virulence factor expression and epithelial invasion by *Candida* species.

25 **Methods and Results:** Plate substrate assays and epithelial models were used to assess *Candida*
26 *albicans* (CCUG 39343 and ATCC 90028) invasion, in conjunction with confocal laser-scanning
27 microscopy and histochemistry. Expression of candidal virulence factors was determined
28 biochemically and by quantitative PCR (qPCR). Changes in surface charge of *C. albicans* following
29 OligoG treatment were analysed using electrophoretic light scattering. OligoG induced marked
30 alterations in hyphal formation in the substrate assays and reduced invasion in the epithelial model
31 ($p < 0.001$). Significant dose-dependent inhibition of phospholipase activity in *C. albicans* was evident
32 following OligoG treatment ($p < 0.05$). Whilst OligoG binding failed to affect alterations in surface-
33 charge ($p > 0.05$), qPCR demonstrated a reduction in phospholipase-B (*PLB2*) and SAPs (*SAP4* and
34 *SAP6*) expression.

35 **Conclusion:** OligoG CF-5/20 reduced *in vitro* virulence factor expression and invasion by *C. albicans*.

36 **Significance and Impact of the Study:** These results, and the previously described potentiation of
37 antifungal activity, define a potential therapeutic opportunity in the treatment of invasive candidal
38 infections.

39

40 **Keywords**

41 Virulence, Biofilms, Antimicrobials, Infection, Fungi

42

43

44

45

46 **Introduction**

47 The incidence of human fungal infections has risen annually with increasing numbers of
48 immunocompromised patients (Miceli *et al.* 2011), in-dwelling prosthetic devices (Chen *et al.* 2011;
49 Silva *et al.* 2012), broad-spectrum antibiotic use and cytotoxic/immunosuppressive therapy. *Candida*
50 species (Pfaller and Diekema 2007) are responsible for >50% of systemic fungal infections (Lass-Floerl
51 2009) and are the most frequently-reported human nosocomial fungal pathogens. In health, *Candida*
52 exist as harmless commensal organisms on the skin-surface, oral mucosa and gastrointestinal tract
53 (Lass-Floerl 2009). *Candida* are, however, opportunistic pathogens in both local- and systemic
54 infection; the latter being associated with both significant mortality (estimated at 30%) (Lass-Floerl
55 2009) and high treatment costs (Ramage *et al.* 2005; Leroy *et al.* 2009).

56 *Candida* readily form biofilms on epithelial and material surfaces which exhibit resistance to
57 antifungals including polyenes and azoles (Kuhn *et al.* 2002). Once a candidal biofilm is formed *in*
58 *vivo*, elimination generally demands removal of the substratum which supports the biofilm. However,
59 removal of medical devices is often impossible, due to the patient's underlying medical condition and/or
60 the anatomic location of the biofilm (Ramage *et al.* 2006). Following adhesion and biofilm formation,
61 the ability of *Candida* (especially *Candida albicans*) to undergo morphological alteration and secrete
62 hydrolytic enzymes facilitates invasion and contributes to their pathogenicity (Mayer *et al.* 2013). The
63 invasion of host-tissue in the pathogenesis of candidal infection is a complex combination of physical,
64 mechanical and enzymatic events, which are both host- and microorganism-dependent. Whilst adhesion
65 to host tissues and morphogenesis contributes to candidal virulence (Yang 2003), virulence factor
66 production is also associated with *Candida* invasion (Shimizu *et al.* 1996).

67 Intact human epithelium acts as a considerable physical and chemical barrier against *Candida*
68 spp. infection. *Candida* spp. possess several discrete mechanisms to increase their dermal
69 pathogenicity, with the expression of surface proteins, e.g. adhesins and invasins facilitating attachment
70 (Nobile *et al.* 2006), and biofilm formation supporting persistence (Finkel and Mitchell 2011).
71 Moreover, yeast-to-hyphal transition facilitates enzymatically-induced tissue invasion (Mayer *et al.*
72 2013), and thigmotropism (contact sensing) directs site-specific invasion (Kumamoto 2008). *Candida*

73 species are highly metabolically adaptable, having the ability to adapt to changes in environmental pH
74 and nutritional availability, as well as having a robust stress-response mechanism (Mayer *et al.* 2013).

75 Secretion of hydrolases is important for the pathogenicity of *C. albicans* and is mediated by
76 three main enzyme classes: secreted aspartyl proteinases (SAPs), phospholipases (PL) and lipases
77 (Mayer *et al.* 2013). Distinct SAPS genes are known to facilitate active penetration of the cross-linked
78 epithelial barrier of the skin (Schaller *et al.* 2000). Increased expression of PL has been associated with
79 antifungal resistance (Ying and Chunyang 2012), whilst secretion of SAPs have been implicated in
80 systemic infections (Sanglard *et al.* 1997).

81 Previous studies demonstrated the ability of a low molecular weight alginate, OligoG CF-5/20
82 (OligoG), to modify bacterial biofilm assembly and reduced resistance to antimicrobial therapy (Khan
83 *et al.* 2012; Powell *et al.* 2013; Roberts *et al.* 2013; Powell *et al.* 2014). More recently, the ability of
84 OligoG to inhibit growth and biofilm formation of *Candida* and *Aspergillus* spp. has been demonstrated
85 (Tøndervik *et al.* 2014). These changes were associated with significantly increased sensitivity to
86 antifungal agents and marked decreases in hyphal formation (Tøndervik *et al.* 2014). The extent to
87 which these changes modulate binding to-, and invasion of, mucosal surfaces by fungal pathogens
88 remains unknown.

89 Candidal adhesion and invasion was investigated using an *in vitro* organotypic keratinocyte
90 model in the presence and absence of OligoG. Substrate assays and real-time PCR were employed to
91 investigate the mechanisms responsible for the observed changes.

92

93 **Materials and methods**

94 **Strains and routine culture media**

95 *C. albicans* CCUG 39343 (clinical isolate) and *C. albicans* ATCC 90028 (reference strain for antifungal
96 susceptibility testing) and *C. glabrata* ATCC 2001 (non-hyphal producing control) were used in this
97 study. *Candida* were grown at 37°C for 18 h on Sabouraud dextrose agar (SDA, Oxoid) or in liquid

98 culture using Sabouraud dextrose broth (SAB, Lab M). The alginate oligomer, OligoG CF-5/20, was
99 prepared as previously described (Khan *et al.* 2012).

100

101 **Growth curves**

102 *C. albicans* ATCC 90028 was grown overnight in Yeast Nitrogen Base (YNB; BD Diagnostics,
103 Cowley, UK) medium supplemented with 0.5% (w/v) glucose at 37°C. The culture was diluted to 5 x
104 10⁶ cells ml⁻¹ and placed in 96-well microtiter plates ± 0.2, 2 and 6% OligoG (w/v) at 37°C for 24 h,
105 with a YNB ± OligoG blank. Optical density was measured at 600 nm (Fluostar Omega plate reader;
106 BMG LABTECH).

107

108 **Hyphal invasion assay**

109 Yeast Peptone Dextrose (YPD) agar was prepared (Roberts and Fink 1994) ± 0.2%, 2% and 6% OligoG.
110 Plates were dried (1 h) at room temperature prior to use. Overnight cultures of *C. albicans* ATCC
111 90028 were grown in YPD broth at 37°C whilst shaking. *Candida* (20 µl ≈ 1x10⁷ cells ml⁻¹ in YPD
112 medium) were deposited on to the YPD agar surface (n=3) and incubated for 72 h at 37°C, followed by
113 72 h at room temperature. Hyphal agar invasion was examined after rinsing the colonies from the agar
114 surface with deionized water (Roberts and Fink 1994). Assays were conducted in triplicate in three,
115 independent, experiments. Photographs employed the same focal length. Agar samples were stained
116 using hematoxylin and eosin (H&E) to study hyphal invasion of the epithelium. Light microscopy
117 images (x100 objective lens) of control and OligoG-treated samples were taken.

118

119 **Reconstituted human epithelium model**

120 Reconstituted human oral epithelium (RHE) tissue was obtained from SkinEthic Laboratories (Nice,
121 France). RHE tissues (n=5) were placed in 6-well tissue culture plates with 1 ml of SkinEthic
122 maintenance medium ± 0.2% OligoG (w/v). *Candida albicans* ATCC 90028, cultured on SDA at 37°C
123 for 24 h, was inoculated into YNB medium supplemented with 0.5% glucose (w/v) for 12 h at 37°C
124 under gentle agitation. The cell-suspension was centrifuged and washed (x3) with phosphate buffered

125 saline (PBS). Following direct counting using a hemocytometer, 50 μl of 2×10^6 cells ml^{-1} was added
126 to the surface of each RHE and incubated for 1, 3, 6 or 12 h at 37°C in a humidified atmosphere with
127 5% CO_2 . Non-infected controls were included in all experiments. The RHE were then rinsed (x2) in
128 PBS to remove planktonic cells and bisected. Half was fixed in 10% (v/v) formalin prior to being
129 embedded in paraffin wax, with the remainder used immediately for LIVE/DEAD® staining (Molecular
130 Probes-Invitrogen, Paisley, UK).

131

132 **Confocal laser scanning LIVE/DEAD® staining of RHE**

133 RHE samples from each time-point were placed on microscope slides and 100 μl of LIVE/DEAD® stain
134 (containing 25 $\mu\text{mol l}^{-1}$ SYTO® 9 and 15 $\mu\text{mol l}^{-1}$ propidium iodide) applied directly to the tissue, as
135 previously described (Boros-Majewska *et al.* 2015). Treated samples were incubated for 30 min at
136 37°C in the dark prior to transfer to clean glass slides. RHE samples were covered with Vectashield®
137 mounting medium and confocal laser scanning microscopy (CLSM) performed (n=3) using a Leica
138 TCS SP2 AOBS spectral confocal microscope (Leica Microsystems GmbH, Wetzlar, Germany).

139

140 **Periodic Acid-Schiff staining**

141 RHE sections (5 μm) were stained using Periodic Acid-Schiff (PAS) stain to study hyphal invasion of
142 the epithelium. Light microscopic images (x100 objective lens) of control and 0.2%-treated OligoG
143 samples (n=144) were taken (10 images/section), and the depth of invasion (≥ 3 per image) was analysed
144 by direct measurement, using ImageJ software.

145

146 **Phospholipase (PL) activity plate assay**

147 *Candida albicans* ATCC 90028 and *C. albicans* CCUG 39343 (with *C. glabrata* ATCC 2001 used as
148 a negative control) were screened for extracellular PL activity after growth on egg-yolk agar
149 (Samaranayake *et al.* 1984). Experiments employed OligoG in the overnight culture medium (prior to
150 inoculation of the egg-yolk agar) and OligoG incorporated into the egg yolk agar at 0.2, 2 and 6% (w/v)
151 without CaCl_2 . Static overnight cultures in SAB were diluted 100-fold into fresh SAB \pm 0.2%, 2% and
152 6% (w/v) OligoG for 18 h at 37°C. A standard inoculum of the test *Candida* (5 $\mu\text{l} \approx 10^7$ cfu ml^{-1}) was

153 deposited onto the egg-yolk agar and dried at room temperature. Plates were incubated at 37°C for 3-
154 7 days; the diameter of the precipitation zone around the colony was then measured (n=3) and PL
155 activity (P_z value) expressed as the ratio of the colony diameter to the total diameter of the colony and
156 precipitation zone (Price *et al.* 1982).

157

158 **Secreted aspartyl protease (SAP) activity plate assay**

159 *Candida albicans* ATCC 90028, *C. albicans* CCUG 39343, and *C. glabrata* ATCC 2001 were screened
160 for SAP production after growth on modified YNB medium (de Menezes Thiele *et al.* 2008). Briefly,
161 1.5% agar (Sigma; w/v) and 0.2% glucose (w/v) was autoclaved followed by the addition of filter
162 sterilized 1.17% YNB without ammonium sulfate, 0.2% bovine serum albumin (Sigma; w/v) and 0.01%
163 Vitox (Oxoid; v/v). The inoculum preparation and analysis was identical to that described in the PL
164 activity assay.

165

166 **Hemolysis plate assay**

167 Sheep-blood SDA, supplemented with 3% glucose, was prepared \pm 0.2%, 2% and 6% OligoG. Static
168 overnight cultures of *C. albicans* CCUG 39343, *C. albicans* ATCC 90028 and *C. glabrata* ATCC 2001
169 were incubated at 37°C in SAB. Cultures were diluted 100-fold into SAB \pm 0.2, 2 and 6% OligoG and
170 re-incubated for 18 h at 37°C. The overnight culture was centrifuged at 2,000 g for 5 min and re-
171 suspended in water to 1×10^7 cells ml⁻¹; a 5 μ l inoculum was placed on each plate (n=3). Plates were
172 incubated at 37°C (48 h) and hemolysis production calculated by dividing the diameter of the colony
173 by the total colony diameter (including the translucent periphery), to determine the hemolytic index, Hi
174 (Yigit *et al.* 2011; Deorukhkar *et al.* 2014). Controls included *Streptococcus pyogenes* (clinical strain;
175 beta hemolytic), *S. pneumoniae* (ATCC 49619; alpha hemolytic) and *Staphylococcus epidermidis*
176 (ATCC 14990; negative control) grown in Mueller-Hinton broth.

177

178 **RNA extraction and Real-Time-PCR (qPCR)**

179 RNA was extracted from *C. albicans* ATCC 90028 cultured as described above. Cultures were adjusted
180 to 1.0×10^8 cells ml⁻¹ in PBS and centrifuged (12000 g, 2 min) before being re-suspended in 0.5 ml

181 RNAlater® and stored at -20°C until required. Cells were pelleted (12000 x g, 2 min) and re-suspended
182 in lysis buffer (RLT buffer, QIAgen, Crawley, UK) containing 1% (v/v) beta-mercaptoethanol. Cells
183 were then lysed using a Mini-Bead-Beater-8 for a total of 4 min (at 2 min intervals with 1 min on ice).
184 Resultant supernatants were transferred to fresh tubes, and the cell-debris pelleted by centrifugation.
185 Total nucleic acid was extracted from the supernatant using 500 µl phenol:chloroform:isoamyl alcohol
186 (25:24:1) (Sigma-Aldrich, Pool, UK). Total RNA was recovered from the aqueous layer after DNase I
187 treatment using the RNeasy Mini Kit (QIAGEN). Gel electrophoresis was used to check purity and
188 integrity of the total RNA, and RNA concentration was measured spectrophotometrically (NanoVue,
189 GE Healthcare, Little Chalfont, UK) and standardized to 300 ng ml⁻¹. Reverse transcription reactions
190 for cDNA synthesis were performed using a total RNA template of (300 ng ml⁻¹), 40 µmol of random
191 nonamer primers (PrimerDesign Ltd) and molecular grade water in a final reaction volume of 10 µl.
192 An annealing step of 5 min at 65°C was performed, samples were cooled on ice and added to the
193 extension mix; 4 µl of 4 x NanoScript2 buffer, 1 µl dNTP mix (10 mM), NanoScript2 enzyme at 1.5 µl
194 (Primer Design, Southampton, UK), and 2.5 µl of molecular grade water and a final volume of 20 µl
195 was incubated at 25°C for 5 min and then at 42°C for 20 min.

196 The primers used in the qPCR analysis were based on previous findings, and are shown in Table
197 1. Primer specificity was tested on extracted genomic DNA. Regions amplified were secreted aspartyl
198 proteinases *SAP4*, *SAP5* and *SAP6* and phospholipases *PLB1* and *PLB2*, with *ACT1* serving as a
199 reference control for *C. albicans*. PCR was performed in 96-well plates in an ABI 7000 instrument
200 (Life Technologies). Each 25 µl reaction contained 2 µl cDNA, 12.5 µl (x2) of SYBR-Green PCR
201 master mix (PrecisionPlus Mastermix; Primer Design, Southampton, UK), 0.5 µl of each primer (10
202 mM), made up to 25 µl with molecular grade water. The thermal cycle profile comprised of initial
203 denaturation at 95°C for 2 min, 40 cycles of denaturation at 95°C for 15s, primer annealing at 58°C for
204 15s, and primer extension at 72°C for 30s. A final extension at 72°C for 2 min was performed, followed
205 by a final cooling step at 4°C. A dissociation stage at 60°C was used to generate a melting-curve for
206 verification of the amplified product. After qPCR, the threshold was adjusted according to the
207 amplification curves of all evaluated genes. Comparison between groups was based on the cycle

208 number at which both the target and reference genes reached threshold cycle (Ct) fluorescence.
209 Analysis of relative gene expression was according to the $\Delta\Delta$ CT method (Bustin *et al.* 2009).

210

211 **Candida cell-surface charge analysis**

212 Zeta-potential analyses were performed using electrophoretic light scattering on *C. albicans* 39343 at
213 pH 5, 7 and 9 and at a salt concentration of 0.01 mol l⁻¹ NaCl. *C. albicans* was grown overnight in SAB
214 at 37°C, and diluted 100-fold in fresh SAB prior to culture at 37°C for 19 h at 80 rev min⁻¹. One ml of
215 the culture was washed in distilled-water (5,500 x g; 3 min). The pellet was re-suspended in 100 µl of
216 0.01 mol l⁻¹ NaCl (pH 5, 7 or 9) and 20 µl added to 1 ml of the buffer ± OligoG (10%) for 20 min; the
217 sample was washed and centrifuged (2,500 x g; 6 min). A Zetasizer Nano ZS (Malvern Instruments)
218 and disposable capillary cells (DTS1061 Malvern instruments) were employed and the resultant zeta
219 potential calculated by applying Smoluchowski's model (Wilson *et al.* 2001).

220

221 **Statistical analysis**

222 GraphPad Prism 3 was used to perform statistical analysis (GraphPad software Inc, California, USA).
223 Measurements of invasion in the PAS-stained RHE images were analysed using a Mann-Whitney test.
224 The data were analyzed by one-way ANOVA followed by a Dunnett Multiple Comparisons test (growth
225 curve, SAP and PL plate assays) and Tukey Kramer multiple comparisons test (real-time PCR data).
226 Data represents the mean in all figures (standard deviation; **Fig. 1-5, S1-S2** and standard error of mean
227 in **Fig. 6**). p<0.05 was considered significant.

228

229 **Results**

230 **OligoG reduced candidal growth**

231 Growth curve studies showed that there was no change in the lag- or exponential-phases when *C.*
232 *albicans* was grown in the presence of OligoG. However, a decrease in optical density was evident at
233 the late-exponential growth phase (>10 h) when samples were treated with ≥2% OligoG (Fig. 1a).

234 OligoG induced a significant dose-dependent reduction in candidal growth compared to the control (at
235 18 h), which was maintained throughout stationary phase (Fig. 1b; $p < 0.05$).

236

237 **OligoG reduced *in vitro* candidal hyphal production and invasion**

238 The hyphal invasion agar assay confirmed that treatment with OligoG ($>0.2\%$) induced a marked dose-
239 dependent decrease in candidal invasion (Fig. 2). A visible reduction in the ability of *C. albicans* to
240 penetrate the agar was seen at increasing OligoG concentrations. H&E stained sections of the agar
241 showed that considerable hyphal invasion was seen in the control samples, and interestingly this often
242 led to a cluster of yeast cells penetrating through the agar along with the hyphae. As the concentration
243 of OligoG increased, less hyphae were visible, with reduced yeast cell clustering within the agar,
244 particularly at OligoG concentrations $\geq 2\%$. Alternatively, hyphal cells may have reverted to yeast cells.

245 Longitudinal CLSM studies of the RHE tissues showed candidal hyphal formation did not occur
246 before 6 h (Fig. 3). However, in contrast to the control in which a vital epithelial layer was evident
247 (depicted by viable green cells), hyphal formation was clearly evident at 6 h on the surface of the
248 inoculated epithelial cells. Moreover, at 12 h, there was an unmistakable further increase in hyphal
249 formation, in conjunction with greater epithelial cell death (red cells). This 12 h time point was
250 therefore chosen as optimal for testing the RHE tissues with OligoG.

251 Fig. 4 shows OligoG-treated RHE sections. An intact epithelium composed of viable (green)
252 keratinocytes in the controls (Fig. 4a), contrasted with increasing numbers of non-viable (red)
253 keratinocytes and abundant hyphal formation in the infected RHE tissues, with a striking decrease in
254 hyphal formation observed in the 0.2% OligoG-treated samples. No change in the ratio of live to dead
255 cells was evident.

256 Quantification of hyphal invasion was conducted using PAS-stained RHE cross-sectional
257 images (Fig. 4b). PAS images demonstrated intact stratified keratinocytes in the uninfected control.
258 However, in the infected control, the stratified layers were clearly infiltrated with hyphae penetrating
259 at least half way through the keratinocyte layers. Quantification of hyphal invasion of the epithelial
260 surface in the RHE model showed a statistically significant reduction in the depth of hyphal invasion
261 observed in the 0.2% OligoG-treated RHE tissues ($p < 0.05$; $n = 144$ measurements of 10 images/section

262 with ≥ 3 measurements of depth of invasion/image) compared to the untreated control, with the hyphae
263 seen predominantly on the tissue surface rather than invading the underlying keratinocytes.

264

265 **Production of the virulence factor phospholipase was reduced in the presence of OligoG**

266 Standard egg-yolk plates showed that phospholipase (PL) production by *C. albicans* ATCC 90028 cells
267 pre-treated with OligoG was significantly decreased, but only at the 5 day time point using 6% OligoG
268 (Fig. 5; $p < 0.05$). Slight strain variations were evident, with no significance seen following OligoG pre-
269 treatment with strain CCUG39343. However, incorporating OligoG into the egg-yolk plates produced
270 a pronounced dose-dependent effect, with significantly decreased production of PL evident at days 3, 5
271 and 7 (at $\geq 2\%$ OligoG; $p < 0.05$; **Fig. 5**) for both strains tested.

272 Analysis of secreted aspartyl protease (SAPs) production showed that treatment of *Candida*
273 with OligoG failed to induce significant differences in hemolytic activity, in either pre-treatment
274 ($p > 0.05$; **Fig. S1a**) or following incorporation of OligoG into the agar ($p > 0.05$; **Fig. S1b**). Unusually,
275 the two *C. albicans* strains tested (ATCC 90028 and CCUG 39343) produced no SAPs in the plate
276 assays, even in untreated controls after 7 day incubations, suggesting that the assay was not sufficiently
277 sensitive.

278

279 **OligoG reduced expression of key phospholipase and secreted aspartyl proteinases**

280 Quantitative RT-PCR demonstrated OligoG induced a decrease in key phospholipase and secreted
281 aspartyl proteinase production at concentrations $\geq 0.2\%$. However, the data only reached statistical
282 significance ($p < 0.05$) for *PLB2*, *SAP4* and *SAP6* expression at 6% OligoG (**Fig. 6**). A dose-dependent
283 decrease in *SAP5* was also evident at 6% OligoG, however this did not reach statistical significance.

284

285 **OligoG did not alter the surface charge of the candidal cell wall**

286 Zeta-potential measurements demonstrated that the surface charge of *Candida* was increased following
287 OligoG treatment, at pH 5 and 7 (not pH 9). Following thorough washing, these changes were not
288 significantly different from the control in any of these test conditions (**Fig. S2**).

289

290 Discussion

291 This study demonstrated the effect of OligoG on the important human fungal pathogen *C. albicans* and
292 showed the ability of this polymer therapy to modify virulence factor production and invasion of *C.*
293 *albicans in vitro*. Numerous *in vivo*, *ex vivo* and *in vitro* models of candidal biofilm formation and
294 invasion have been developed. Whilst no single *in vitro* model of *Candida* infection exists, numerous
295 studies have employed this RHE model (de Fraissinette *et al.* 1999) which, although lacking any
296 immunological component, has been extensively used to study *Candida*/keratinocyte
297 interactions/invasion at the gene, protein and cellular level (Schaller *et al.* 2001; Schaller *et al.* 2002;
298 Bartie *et al.* 2004; Jayatilake *et al.* 2005; Malic *et al.* 2007). Although authors have criticized the model
299 (Murdoch *et al.* 2005; Colley *et al.* 2011; Yadev *et al.* 2011) it is still useful as it allows the early events
300 of fungal pathogenesis *i.e.* adhesion to the keratinocyte surface and initial invasion of the insoluble
301 keratinocyte barrier of cross-linked proteins and lipids (Schaller *et al.* 2006) to be studied. Researchers
302 have also shown how strain-dependent invasiveness in the RHE may reflect pathogenicity *in vivo* (Malic
303 *et al.* 2007). It should also be borne in mind that in the early stages of pathogenesis, keratinocytes (via
304 this physical barrier and their expression of cytokines and Toll-like receptors) represent an important
305 element of the dermal innate immune response to fungal and many other pathogens (Mogensen 2009).

306 Imaging revealed that no candidal hyphal infiltration was evident at <6 h. Beyond 6 h however,
307 adherence and hyphal formation were clearly evident. At 12 h, LIVE/DEAD® staining demonstrated
308 markedly decreased hyphal formation on the surface of the OligoG-treated RHE models, with few actual
309 hyphae visible in contrast to the abundant hyphae present in the untreated control. Whilst these results
310 may appear to contrast with the growth inhibition described in previous studies, these were not however,
311 apparent at early time points ≤ 12 h; the previously-described differences being evident only at 48 h
312 (Tøndervik *et al.* 2014).

313 Whilst attachment, proliferation and biofilm assembly are important in colonization of the
314 epithelial surface, invasion is a key pathogenic phenotype in candidal pathogenesis (Bartie *et al.* 2004;
315 Mayer *et al.* 2013). Invasion studies here employed cross-sectional imaging of RHE as previously
316 utilized in virulence studies of clinical *Candida* isolates (Malic *et al.* 2007; Boros-Majewska *et al.*

317 2014), which revealed that OligoG was not fungicidal (as ascertained by the absence of red-stained,
318 non-vital cells), differential quantification of samples, as previously described by Boros-Majewska *et*
319 *al.* (2014), could not be employed. Analysis of invasion in the RHE and agar model systems revealed
320 that whilst no differences in fungal viability were evident, OligoG treatment induced markedly reduced
321 invasion in both model systems, with a dose-dependent decrease in hyphal formation being evident in
322 the agar model. Interestingly at high concentrations of OligoG (>6%) in the agar model, addition of the
323 alginate oligomers reduced the structural integrity of the agar. The decreased invasion, therefore, did
324 not reflect the OligoG induced alteration in physical density of the media. The findings in the RHE
325 model were in line with the reduced *Candida* growth demonstrated in the presence of OligoG. It should
326 be noted that the use of higher concentrations of OligoG (>2%) was not possible in this system as higher
327 concentrations impaired both direct visualization and the cellular viability of the epithelial component
328 of the superficial keratinocyte layer, in this (avascular) air-liquid interface model. This effect on
329 keratinocyte viability is a particular feature of this model and has not been observed in the extensive
330 pre-clinical (*in vitro*), animal, and human clinical testing of chronically-inhaled OligoG prior to EMA
331 and FDA approval (Pritchard *et al.* 2016).

332 Dermal invasion by *Candida* is facilitated by production of a heterogeneous group of
333 hydrolytic enzymes (Schaller *et al.* 2005). SAPs are believed to mediate *Candida* invasion of epithelial
334 cells, with *SAP5* in particular, also strongly associated with proteolytic degradation of E-cadherin found
335 in the intracellular junctions of keratinocytes (Villar *et al.* 2007). Interestingly, as keratinocyte damage
336 is not prevented by pepstatin A (which partially inhibits invasion), other mechanisms are, therefore,
337 clearly important (Naglik *et al.* 2008). *SAPs 1-3* have been shown to have a direct role in the tissue
338 damage of superficial infection whilst *SAPs 4-6* are important for invasion and interaction with
339 components of cellular defense (Schaller *et al.* 2001) and yeast to hypha transition (Naglik *et al.* 2003).
340 A reduction in *SAP4-6* in the presence of OligoG (being significant for *SAP 4* and *6*) could explain the
341 corresponding decrease in hyphal formation and invasion. However, the pathogenicity of SAPs remains
342 contentious (Correia *et al.* 2010) with poor correlation found between individual *SAP* gene-expression
343 and epithelial damage (Naglik *et al.* 2008). *SAP* expression is also dependent on environmental pH
344 (Staib *et al.* 2000), therefore, it is unsurprising that *SAP* production in *C. albicans* was not detected

345 phenotypically in this study. The marked reductions in hyphal formation, which were induced by
346 OligoG, were reflected in alterations in the gene expression of *PLB2*, *SAP4* and *SAP6*, evident by qPCR
347 analysis. The lower expression of PLs and SAPs in the RHE model system may reflect their decreased
348 expression in established laboratory isolates, and the reduced sensitivity of the plate-based assay in
349 comparison to the qPCR (Boriollo *et al.* 2009).

350 The effects of OligoG on hyphal formation and fungal invasion in the RHE model reflected its
351 previously reported reduction of germ-tube formation *in vitro* (Tøndervik *et al.* 2014). *In vivo*, invasion
352 is not only mediated by hydrolytic enzymes, but may be potentiated by synergistic interactions with
353 other bacterial species on the skin or mucosal surfaces e.g. *Staphylococcus* (Zago *et al.* 2015) and
354 *Streptococcus* spp. (Bamford *et al.* 2009). *SAPs 4-6* were investigated due to their involvement in
355 systemic infections (Malic *et al.* 2007). *SAP 4-6* are hyphal-specific; their expression being associated
356 with invasive candidal strains. It has recently been suggested that the importance of SAPs may be an
357 over-stated epiphenomenon in *ex-vivo* systems, reflecting experimental conditions, rather than
358 pathological invasion *in vivo* (Naglik *et al.* 2008). Both *SAPs 1-3* and *SAPs 4-6* subfamilies were
359 reported to be lower when analysed using qPCR in the RHE model, indicating that SAP production
360 needs to be further analysed *in vivo* (Naglik *et al.* 2008).

361 *C. albicans* is known to possess up to five extracellular phospholipases (*PLB1-5*) which may
362 also play a role in virulence, possibly via disruption of the host membrane (Mayer *et al.* 2013). PL
363 activity represents an important virulence factor in not only *Candida*, but also in a range of other fungi
364 including *Aspergillus* (Alp and Arikan 2008), *Cryptococcus* (Ganendren *et al.* 2006) and bacteria such
365 as *Clostridium perfringens* and *Pseudomonas aeruginosa* (Ghannoum 2000). Candidal PLs are a
366 heterogeneous group of important enzymes associated with invasion (Ghannoum 2000) and expression
367 is localized to the peripheries of the hyphal tips and initial sites of bud- formation (Jayatilake *et al.*
368 2005) (where they act as a mechanical anchor for yeast survival on the keratinocyte surface). PL
369 expression is reduced in non-hyphal forming species e.g. *C. glabrata* (Kantarcioglu and Yucel 2002)
370 and are believed to modify host transduction pathways, perturb cell signaling (Oishi *et al.* 1988) and
371 local immune responses (Soares *et al.* 2010). Whilst PL expression has however previously been shown

372 not to correlate with RHE invasion in this model (Malic *et al.* 2007) it was interesting that the reduced
373 hyphal formation and invasion induced by OligoG was associated with a significant decrease in Plb2.

374 Studies of the interaction of OligoG with the *Candida* cell wall were deemed important as
375 alterations in pseudomonal bacterial (and biofilm) behavior had previously been shown related to
376 bacterial cell-surface binding and modification of cell-surface charge by long-range forces (which
377 determine pathogen/host cell interactions) (Powell *et al.* 2014). Interestingly, whilst ELS experiments
378 with *P. aeruginosa* showed how alginate oligomers bound tightly to the bacterial cell surface and resist
379 hydrodynamic shear, in *Candida* no such changes were apparent. Treated candidal specimens also
380 failed to demonstrate the “clumping”/aggregation previously observed in *P. aeruginosa* biofilms. These
381 findings reflect the contrasting nature of the yeast cell wall (composed of glucan, chitin and
382 mannoproteins), with that of the lipid-rich pseudomonal outer membrane incorporating both
383 peptidoglycan and lipopolysaccharide (Hawrani *et al.* 2010).

384 In conclusion, these studies have demonstrated the ability of the alginate oligosaccharide
385 OligoG CF-5/20, to modify virulence factor expression in *Candida* and inhibit hyphal formation and
386 invasion. The observed reduction in hyphal infiltration reflected reductions in hydrolytic enzyme
387 production. These findings demonstrate direct and indirect mechanisms by which OligoG may
388 influence candidal invasion and be of potential utility in the management of fungal pathogens in human
389 disease.

390

391 **Acknowledgments**

392 For *Candida* strains we thank Prof. David W. Williams (Cardiff University) and Dr. Mariana Henriques
393 (Minho University, Portugal). We thank Mrs Kath Allsop and Mrs Sue Wozniak for preparing the H&E
394 and PAS samples. The funders had no role in the study-design, data collection and interpretation, or
395 the decision to submit the work for publication. This work was supported by the European Union via
396 Knowledge Economy Skills Scholarships programme (grant number ESF 2007-2013 80300); the
397 Research Council of Norway (grant number 228542/O30); Cystic Fibrosis Foundation US (grant
398 number ALGIPHARMAIIWO) and AlgiPharma AS.

400 **Conflict of interest**

401 D.W.T. has a consultancy relationship and has, with K.E.H., received research funding from
402 AlgiPharma AS. P.D.R. is the R&D director of AlgiPharma AS. The other authors have no conflicts
403 of interest to disclose.

404

405 **References**

406 Alp, S. and Arikan, S. (2008) Investigation of extracellular elastase, acid proteinase and
407 phospholipase activities as putative virulence factors in clinical isolates of *Aspergillus* species. *J Basic*
408 *Microbiol* **48**, 331-337.

409 Bamford, C.V., d'Mello, A., Nobbs, A.H., Dutton, L.C., Vickerman, M.M. and Jenkinson, H.F. (2009)
410 *Streptococcus gordonii* modulates *Candida albicans* biofilm formation through intergeneric
411 communication. *Infect Immun* **77**, 3696-3704.

412 Bartie, K.L., Williams, D.W., Wilson, M.J., Potts, A.J.C. and Lewis, M.A.O. (2004) Differential
413 invasion of *Candida albicans* isolates in an in vitro model of oral candidosis. *Oral Microbiol Immunol*
414 **19**, 293-296.

415 Boriollo, M.F.G., Bassi, R.C., dos Santos Nascimento, C.M.G., Feliciano, L.M., Francisco, S.B.,
416 Barros, L.M., Spolidorio, L.C. and Palomari Spolidorio, D.M. (2009) Distribution and hydrolytic
417 enzyme characteristics of *Candida albicans* strains isolated from diabetic patients and their non-
418 diabetic consorts. *Oral Microbiol Immunol* **24**, 437-450.

419 Boros-Majewska, J., Salewska, N., Borowski, E., Milewski, S., Malic, S., Wei, X.Q., Hayes, A.J.,
420 Wilson, M.J. and Williams, D.W. (2014) Novel Nystatin A(1) derivatives exhibiting low host cell
421 toxicity and antifungal activity in an *in vitro* model of oral candidosis. *Med Microbiol Immunol* **203**,
422 341-355.

423 Boros-Majewska, J., Turczyk, L., Wei, X., Milewski, S. and Williams, D.W. (2015) A novel *in vitro*
424 assay for assessing efficacy and toxicity of antifungals using human leukaemic cells infected with
425 *Candida albicans*. *J Appl Microbiol* **119**, 177-187.

426 Bustin, S.A., Benes, V., Garson, J.A., Hellemans, J., Huggett, J., Kubista, M., Mueller, R., Nolan, T.,
427 Pfaffl, M.W., Shipley, G.L., Vandesompele, J. and Wittwer, C.T. (2009) The MIQE Guidelines:
428 Minimum Information for Publication of Quantitative Real-Time PCR Experiments. *Clin Chem* **55**,
429 611-622.

430 Cavalcanti, Y.W., Morse, D.J., da Silva, W.J., Del-Bel-Cury, A.A., Wei, X., Wilson, M., Milward, P.,
431 Lewis, M., Bradshaw, D. and Williams, D.W. (2015) Virulence and pathogenicity of *Candida*
432 *albicans* is enhanced in biofilms containing oral bacteria. *Biofouling* **31**, 27-38.

433 Chen, S.C.A., Lewis, R.E. and Kontoyiannis, D.P. (2011) Direct effects of non-antifungal agents used
434 in cancer chemotherapy and organ transplantation on the development and virulence of *Candida* and
435 *Aspergillus* species. *Virulence* **2**, 280-295.

436 Colley, H.E., Hearnden, V., Jones, A.V., Weinreb, P.H., Violette, S.M., MacNeil, S., Thornhill, M.H.
437 and Murdoch, C. (2011) Development of tissue-engineered models of oral dysplasia and early
438 invasive oral squamous cell carcinoma. *Br J Cancer* **105**, 1582-1592.

439 Correia, A., Lermann, U., Teixeira, L., Cerca, F., Botelho, S., Gil da Costa, R.M., Sampaio, P.,
440 Gaertner, F., Morschhauser, J., Vilanova, M. and Pais, C. (2010) Limited role of secreted aspartyl
441 proteinases Sap1 to Sap6 in *Candida albicans* virulence and host immune response in murine
442 hematogenously disseminated Candidiasis. *Infect Immun* **78**, 4839-4849.

443 de Fraissinette, A.D., Picarles, V., Chibout, S., Kolopp, M., Medina, J., Burtin, P., Ebelin, M.E.,
444 Osborne, S., Mayer, F.K., Spake, A., Rosdy, M., De Wever, B., Ettlin, R.A. and Cordier, A. (1999)
445 Predictivity of an *in vitro* model for acute and chronic skin irritation (SkinEthic) applied to the testing
446 of topical vehicles. *Cell Biol Toxicol* **15**, 121-135.

447 de Menezes Thiele, M.C., de Paula e Carvalho, A., Gursky, L.C., Rosa, R.T., Samaranayake, L.P. and
448 Ribeiro Rosa, E.A. (2008) The role of candidal histolytic enzymes on denture-induced stomatitis in
449 patients living in retirement homes. *Gerodontology* **25**, 229-236.

450 Deorukhkar, S.C., Saini, S. and Mathew, S. (2014) Virulence factors contributing to pathogenicity of
451 *Candida tropicalis* and its antifungal susceptibility profile. *Int J Med Microbiol* **2014**, 456878-
452 456878.

453 Finkel, J.S. and Mitchell, A.P. (2011) Genetic control of *Candida albicans* biofilm development. *Nat*
454 *Rev Microbiol* **9**, 109-118.

455 Ganendren, R., Carter, E., Sorrell, T., Widmer, F. and Wright, L. (2006) Phospholipase B activity
456 enhances adhesion of *Cryptococcus neoformans* to a human lung epithelial cell line. *Microbes Infect*
457 **8**, 1006-1015.

458 Ghannoum, M.A. (2000) Potential role of phospholipases in virulence and fungal pathogenesis. *Clin*
459 *Microbiol Rev* **13**, 122-43.

460 Hawrani, A., Howe, R.A., Walsh, T.R. and Dempsey, C.E. (2010) Thermodynamics of RTA3 peptide
461 binding to membranes and consequences for antimicrobial activity. *Biochim Biophys Acta-Biomembr*
462 **1798**, 1254-1262.

463 Jayatilake, J., Samaranayake, Y.H. and Samaranayake, L.P. (2005) An ultrastructural and a
464 cytochemical study of candidal invasion of reconstituted human oral epithelium. *J Oral Pathol Med*
465 **34**, 240-246.

466 Kantarcioglu, A.S. and Yucel, A. (2002) Phospholipase and protease activities in clinical *Candida*
467 isolates with reference to the sources of strains. *Mycoses* **45**, 160-165.

468 Khan, S., Tondervik, A., Sletta, H., Klinkenberg, G., Emanuel, C., Onsoyen, E., Myrvold, R., Howe,
469 R.A., Walsh, T.R., Hill, K.E. and Thomas, D.W. (2012) Overcoming drug resistance with alginate

470 oligosaccharides able to potentiate the action of selected antibiotics. *Antimicrob Agents Chemother*
471 **56**, 5134-5141.

472 Kuhn, D.M., George, T., Chandra, J., Mukherjee, P.K. and Ghannoum, M.A. (2002) Antifungal
473 susceptibility of *Candida* biofilms: Unique efficacy of amphotericin B lipid formulations and
474 echinocandins. *Antimicrob Agents Chemother* **46**, 1773-1780.

475 Kumamoto, C.A. (2008) Molecular mechanisms of mechanosensing and their roles in fungal contact
476 sensing. *Nat Rev Microbiol* **6**, 667-673.

477 Lass-Floerl, C. (2009) The changing face of epidemiology of invasive fungal disease in Europe.
478 *Mycoses* **52**, 197-205.

479 Leroy, O., Gangneux, J.-P., Montravers, P., Mira, J.-P., Gouin, F., Sollet, J.-P., Carlet, J., Reynes, J.,
480 Rosenheim, M., Regnier, B., Lortholary, O. and AmarCand Study, G. (2009) Epidemiology,
481 management, and risk factors for death of invasive *Candida* infections in critical care: A multicenter,
482 prospective, observational study in France (2005-2006). *Crit Care Med* **37**, 1612-1618.

483 Malic, S., Hill, K.E., Ralphs, J.R., Hayes, A., Thomas, D.W., Potts, A.J. and Williams, D.W. (2007)
484 Characterization of *Candida albicans* infection of an in vitro oral epithelial model using confocal
485 laser scanning microscopy. *Oral Microbiol Immunol* **22**, 188-194.

486 Mayer, F.L., Wilson, D. and Hube, B. (2013) *Candida albicans* pathogenicity mechanisms. *Virulence*
487 **4**, 119-128.

488 Miceli, M.H., Diaz, J.A. and Lee, S.A. (2011) Emerging opportunistic yeast infections. *Lancet Infect*
489 *Dis* **11**, 142-151.

490 Mogensen, T.H. (2009) Pathogen recognition and inflammatory signaling in innate immune defenses.
491 *Clin Microbiol Rev* **22**, 240-273.

492 Monod, M., Hube, B., Hess, D. and Sanglard, D. (1998) Differential regulation of SAP8 and SAP9,
493 which encode two new members of the secreted aspartic proteinase family in *Candida albicans*.
494 *Microbiol-UK* **144**, 2731-2737.

495 Monod, M., Togni, G., Hube, B. and Sanglard, D. (1994) Multiplicity of genes encoding secreted
496 aspartic proteinases in *Candida* species. *Mol Microbiol* **13**, 357-368.

497 Murdoch, C., Muthana, M. and Lewis, C.E. (2005) Hypoxia regulates macrophage functions in
498 inflammation. *J Immunol* **175**, 6257-6263.

499 Naglik, J.R., Challacombe, S.J. and Hube, B. (2003) *Candida albicans* secreted aspartyl proteinases in
500 virulence and pathogenesis. *Microbiol Mol Biol Rev* **67**, 400-428.

501 Naglik, J.R., Moyes, D., Makwana, J., Kanzaria, P., Tsihlaki, E., Weindl, G., Tappuni, A.R.,
502 Rodgers, C.A., Woodman, A.J., Challacombe, S.J., Schaller, M. and Hube, B. (2008) Quantitative
503 expression of the *Candida albicans* secreted aspartyl proteinase gene family in human oral and
504 vaginal candidiasis. *Microbiol-SGM* **154**, 3266-3280.

505 Niewerth, M. and Korting, H.C. (2001) Phospholipases of *Candida albicans*. *Mycoses* **44**, 361-367.

506 Nobile, C.J., Nett, J.E., Andes, D.R. and Mitchell, A.P. (2006) Function of *Candida albicans* adhesin
507 Hwp1 in biofilm formation. *Eukaryot Cell* **5**, 1604-1610.

508 Oishi, K., Raynor, R.L., Charp, P.A. and Kuo, J.F. (1988) Regulation of protein kinase C by
509 lysophospholipids. Potential role in signal transduction. *J Biol Chem* **263**, 6865-6871.

510 Pfaller, M.A. and Diekema, D.J. (2007) Epidemiology of invasive candidiasis: a persistent public
511 health problem. *Clin Microbiol Rev* **20**, 133-163.

512 Powell, L.C., Pritchard, M.F., Emanuel, C., Onsoyen, E., Rye, P.D., Wright, C.J., Hill, K.E. and
513 Thomas, D.W. (2014) A nanoscale characterization of the interaction of a novel alginate oligomer
514 with the cell surface and motility of *Pseudomonas aeruginosa*. *A J Respir Cell Mol Biol* **50**, 483-492.

515 Powell, L.C., Sowedan, A., Khan, S., Wright, C.J., Hawkins, K., Onsoyen, E., Myrvold, R., Hill, K.E.
516 and Thomas, D.W. (2013) The effect of alginate oligosaccharides on the mechanical properties of
517 Gram-negative biofilms. *Biofouling* **29**, 413-421.

518 Price, M.F., Wilkinson, I.D. and Gentry, L.O. (1982) Plate method for detection of phospholipase
519 activity in *Candida albicans*. *J Med Vet Mycol* **20**, 7-14.

520 Pritchard, M.F., Powell, L.C., Menzies, G.E., Lewis, P.D., Hawkins, K., Wright, C., Doull, I., Walsh,
521 T.R., Onsoyen, E., Dessen, A., Myrvold, R., Rye, P.D., Myrset, A.H., Stevens, H.N.E., Hodges, L.A.,
522 MacGregor, G., Neilly, J.B., Hill, K.E. and Thomas, D.W. (2016) A new class of safe oligosaccharide
523 polymer therapy to modify the mucus barrier of chronic respiratory disease. *Mol Pharma* **13**, 863-872.

524 Ramage, G., Martinez, J.P. and Lopez-Ribot, J.L. (2006) *Candida* biofilms on implanted biomaterials:
525 a clinically significant problem. *FEMS Yeast Res* **6**, 979-986.

526 Ramage, G., Saville, S.P., Thomas, D.P. and Lopez-Ribot, J.L. (2005) *Candida* biofilms: an update.
527 *Eukaryot Cell* **4**, 633-638.

528 Roberts, J.L., Khan, S., Emanuel, C., Powell, L.C., Pritchard, M.F., Onsoyen, E., Myrvold, R.,
529 Thomas, D.W. and Hill, K.E. (2013) An *in vitro* study of alginate oligomer therapies on oral biofilms.
530 *J Dent* **41**, 892-899.

531 Roberts, R.L. and Fink, G.R. (1994) Elements of a single MAP kinase cascade in *Saccharomyces*
532 *cerevisiae* mediate two developmental programs in the same cell type: mating and invasive growth.
533 *Genes Dev* **8**, 2974-2985.

534 Samaranayake, L.P., Raeside, J.M. and Macfarlane, T.W. (1984) Factors affecting the phospholipase
535 activity of *Candida* species *in vitro*. *J Med Vet Mycol* **22**, 201-207.

536 Sanglard, D., Hube, B., Monod, M., Odds, F.C. and Gow, N.A.R. (1997) A triple deletion of the
537 secreted aspartyl proteinase genes SAP4, SAP5, and SAP6 of *Candida albicans* causes attenuated
538 virulence. *Infect Immun* **65**, 3539-3546.

539 Schaller, M., Borelli, C., Korting, H.C. and Hube, B. (2005) Hydrolytic enzymes as virulence factors
540 of *Candida albicans*. *Mycoses* **48**, 365-377.

541 Schaller, M., Januschke, E., Schackert, C., Woerle, B. and Korting, H.C. (2001) Different isoforms of
542 secreted aspartyl proteinases (Sap) are expressed by *Candida albicans* during oral and cutaneous
543 candidosis *in vivo*. *J Med Microbiol* **50**, 743-747.

544 Schaller, M., Mailhammer, R., Grassl, G., Sander, C.A., Hube, B. and Korting, H.C. (2002) Infection
545 of human oral epithelia with *Candida* species induces cytokine expression correlated to the degree of
546 virulence. *J Invest Dermatol* **118**, 652-657.

547 Schaller, M., Schackert, C., Korting, H.C., Januschke, E. and Hube, B. (2000) Invasion of *Candida*
548 *albicans* correlates with expression of secreted aspartic proteinases during experimental infection of
549 human epidermis. *J Invest Dermatol* **114**, 712-717.

550 Schaller, M., Zakikhany, K., Naglik, J.R., Weindl, G. and Hube, B. (2006) Models of oral and vaginal
551 candidiasis based on *in vitro* reconstituted human epithelia. *Nat Protoc* **1**, 2767-2773.

552 Shimizu, M.T., Almeida, N.Q., Fantinato, V. and Unterkircher, C.S. (1996) Studies on hyaluronidase,
553 chondroitin sulphatase, proteinase and phospholipase secreted by *Candida* species. *Mycoses* **39**, 161-
554 167.

555 Silva, S., Negri, M., Henriques, M., Oliveira, R., Williams, D.W. and Azeredo, J. (2012) *Candida*
556 *glabrata*, *Candida parapsilosis* and *Candida tropicalis*: biology, epidemiology, pathogenicity and
557 antifungal resistance. *FEMS Microbiol Rev* **36**, 288-305.

558 Soares, D.A., de Andrade, R.V., Silva, S.S., Bocca, A.L., Soares Felipe, S.M. and Petrofeza, S. (2010)
559 Extracellular *Paracoccidioides brasiliensis* phospholipase B involvement in alveolar macrophage
560 interaction. *Bmc Microbiol* **10**, 241.

561 Staib, P., Kretschmar, M., Nichterlein, T., Hof, H. and Morschhauser, J. (2000) Differential activation
562 of a *Candida albicans* virulence gene family during infection. *Proc Natl Acad Sci USA* **97**, 6102-
563 6107.

564 Sugiyama, Y., Nakashima, S., Mirbod, F., Kanoh, H., Kitajima, Y., Ghannoum, M.A. and Nozawa, Y.
565 (1999) Molecular cloning of a second phospholipase B gene, caPLB2 from *Candida albicans*. *Med*
566 *Mycol* **37**, 61-67.

567 Tøndervik, A., Sletta, H., Klinkenberg, G., Emanuel, C., Powell, L.C., Pritchard, M.F., Khan, S.,
568 Craine, K.M., Onsøyen, E., Rye, P.D., Wright, C., Thomas, D.W. and Hill, K.E. (2014) Alginate
569 oligosaccharides inhibit fungal cell growth and potentiate the activity of antifungals against *Candida*
570 and *Aspergillus* spp. *Plos One* **9**, e112518.

571 Villar, C.C., Kashleva, H., Nobile, C.J., Mitchell, A.P. and Dongari-Bagtzoglou, A. (2007) Mucosal
572 tissue invasion by *Candida albicans* is associated with E-cadherin degradation, mediated by
573 transcription factor Rim101p and protease Sap5p. *Infect Immun* **75**, 2126-2135.

574 Wilson, W.W., Wade, M.M., Holman, S.C. and Champlin, F.R. (2001) Status of methods for
575 assessing bacterial cell surface charge properties based on zeta potential measurements. *J Microbiol*
576 *Methods* **43**, 153-164.

577 Yadev, N.R., Murdoch, C., Saville, S.P. and Thornhill, M.H. (2011) Evaluation of tissue engineered
578 models of the oral mucosa to investigate oral candidiasis. *Microb Pathog* **50**, 278-285.

579 Yang, Y.L. (2003) Virulence factors of *Candida* species. *J Microbiol Immunol Infect* **36**, 223-228.

580 Yigit, N., Aktas, E., Dagistan, S. and Ayyildiz, A. (2011) Investigating biofilm production, coagulase
581 and hemolytic activity in *Candida* species isolated from denture stomatitis patients. *Eurasian J Med*
582 **43**, 27-32.

583 Ying, S. and Chunyang, L. (2012) Correlation between phospholipase of *Candida albicans* and
584 resistance to fluconazole. *Mycoses* **55**, 50-55.

585 Zago, C.E., Silva, S., Sanita, P.V., Barbugli, P.A., Improta Dias, C.M., Lordello, V.B. and Vergani,
586 C.E. (2015) Dynamics of biofilm formation and the interaction between *Candida albicans* and
587 methicillin-susceptible (MSSA) and -resistant *Staphylococcus aureus* (MRSA). *Plos One* **10**,
588 e0123206.

589 **Table 1** Primers used for quantitative PCR.

Target gene	Additional information	Forward primer (5' - 3')	Reverse primer (5' - 3')	Reference
<i>SAP4</i>	Secreted aspartyl proteinase	AATGATGTGGGCAAAGAGG	ACACCACCAATACCAACGGT	(Monod <i>et al.</i> 1994; Monod <i>et al.</i> 1998)
<i>SAP5</i>	Secreted aspartyl proteinase	ATTAATTGATGCGGCTCCAG	ACACCACCAATACCAACGGT	(Monod <i>et al.</i> 1994; Monod <i>et al.</i> 1998)
<i>SAP6</i>	Secreted aspartyl proteinase	TCCAAACCAACGAAGCTACC	GCAGGAACGGAGATCTTGAG	(Monod <i>et al.</i> 1994; Monod <i>et al.</i> 1998)
<i>PLB1</i>	Phospholipase B	CAACGAAGCGGTGTTGTCTA	TTGCTGCCAGAACTTTTGAA	(Sugiyama <i>et al.</i> 1999; Niewerth and Korting 2001)
<i>PLB2</i>	Phospholipase B	GGCCAGATGGATCAGCTTTA	AAGTTCTGGGCATCACATCC	(Sugiyama <i>et al.</i> 1999; Niewerth and Korting 2001)
<i>ACT1</i>	<i>C. albicans</i> actin reference gene	TGCTGAACGTATGCAAAAGG	TGAACAATGGATGGACCAGA	(Cavalcanti <i>et al.</i> 2015)

590

591 **Figure legends**

592 **Figure 1** Growth of *C. albicans* in the presence of OligoG. Growth curves of *Candida albicans* ATCC
593 90028 (n=3) ± OligoG at 0% (○), 0.2% (□), 2% (●), 6% (■) over 24 h grown in SAB (a) Representative
594 growth curves. (b) Mean optical density at 18 h time point (n=3; *p<0.05).

595

596 **Figure 2** Agar hyphal invasion model of *C. albicans* in the presence of OligoG. Yeast Peptone Dextrose
597 agar plate assay ± OligoG (0.2%, 2% and 6%) showing hyphal invasion with corresponding light
598 microscopy H&E stained images of cross-sectional agar slices (x20).

599

600 **Figure 3** Epithelial attachment of *Candida* in the RHE model. Time dependent invasion model showing
601 LIVE/DEAD® CLSM images of RHE samples infected with *C. albicans* ATCC 90028 (2×10^6 cfu ml⁻¹)
602 for 1, 3, 6 and 12 h, scale bar 40 μm.

603

604 **Figure 4** Imaging and quantification of OligoG treated *C. albicans* hyphal invasion in RHE. CLSM
605 images of RHE samples infected with *C. albicans* ATCC 90028 for 12 h. (a) LIVE/DEAD® staining,
606 scale bar 40μm; (b) Periodic acid–Schiff staining of fixed RHE samples (blue) infected with *C. albicans*
607 ATCC 90028 (purple) and boxplot of hyphal invasion measurements (n=64; *p< 0.05).

608

609 **Figure 5** Phospholipase production of *C. albicans* in the presence of OligoG. *C. albicans* ATCC 90028
610 and CCUG 39343 phospholipase plate assay ± OligoG in the overnight broth or agar (0.2%, 2% and
611 6%) for 3 days (white), 5 days (grey) and 7 days (black) showing actual Pz values (*p< 0.05; n=3). Pz
612 of 1.0 = no phospholipase activity.

613

614 **Figure 6** Molecular quantification of hydrolytic enzyme production of *C. albicans* in the presence of
615 OligoG. Relative gene expression of phospholipase B (*PLB1*, *PLB2*) and secreted aspartyl proteinases
616 (*SAPs 4, 5 and 6*) following *C. albicans* ATCC 90028 treatment with OligoG (n=3; *p<0.05).

617

618 **Supporting information**

619 **Figure S1** *C. albicans* ATCC 90028 hemolysis agar plate assay \pm OligoG 0.2%, 2% and 6% (a) in broth
620 or (b) in agar.

621 **Figure S2** Mean Zeta Potential (mV) values for *C. albicans* CCUG 39343; untreated *Candida* (pre-
622 wash), treated *Candida* with 10% OligoG (pre-wash), untreated *Candida* (post-wash) and treated
623 *Candida* with 10% OligoG (post-wash) at 0.01 mol l⁻¹ NaCl, pH 5, 7 and 9. (^ false positive result).

624

625

626

627

628

629

630

631

632

633

634

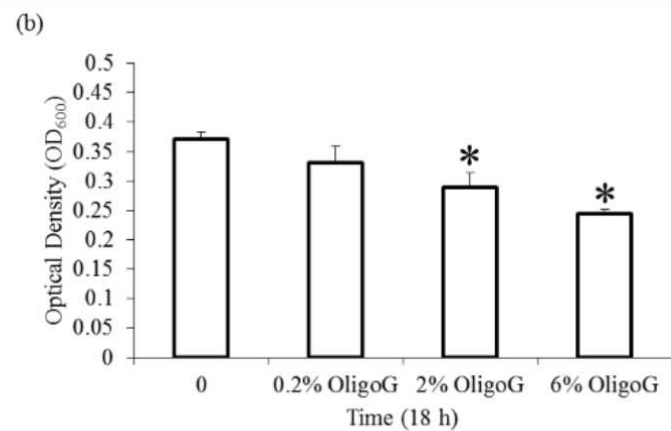
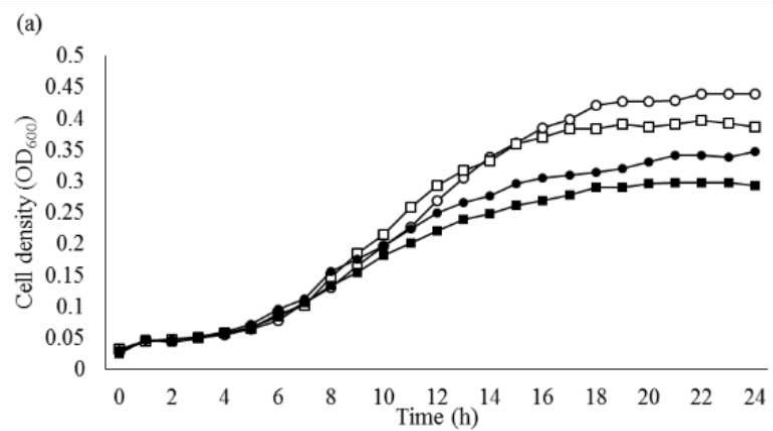
635

636

637

638 **Figure 1**

639



640

641

642

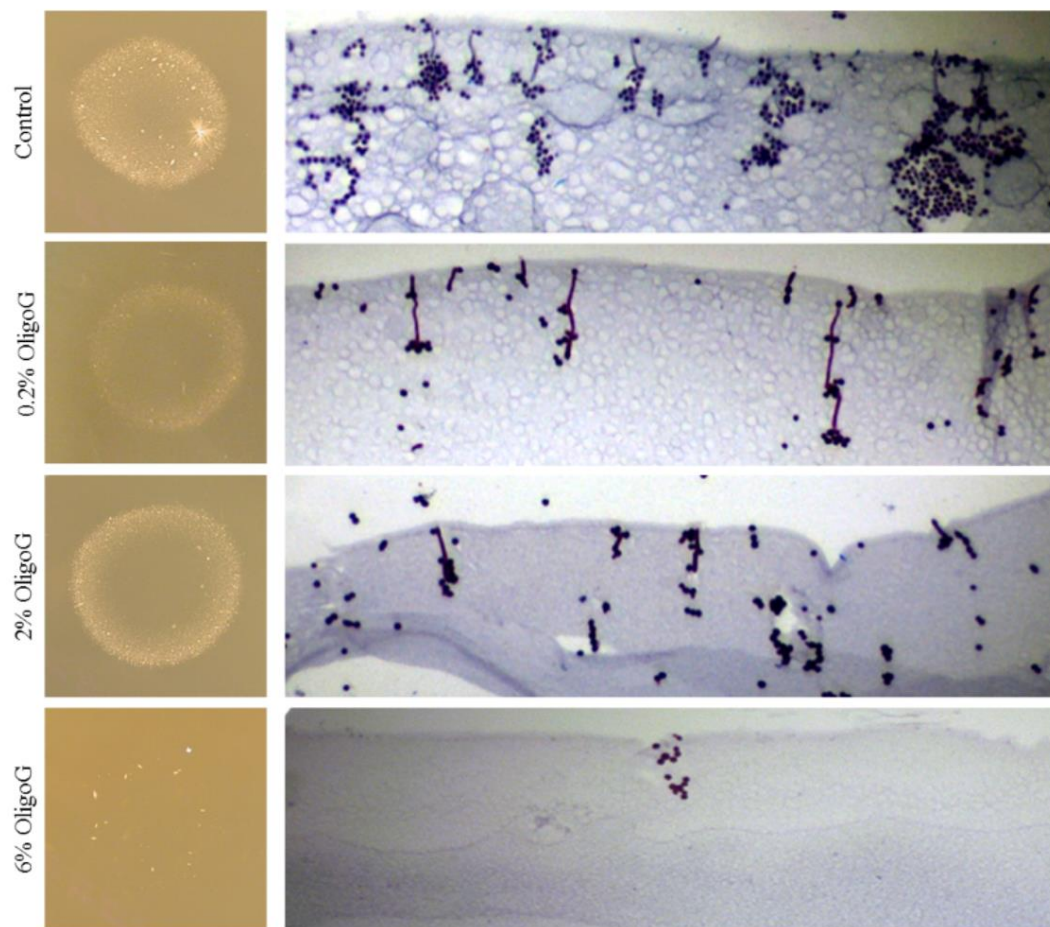
643

644

645

646

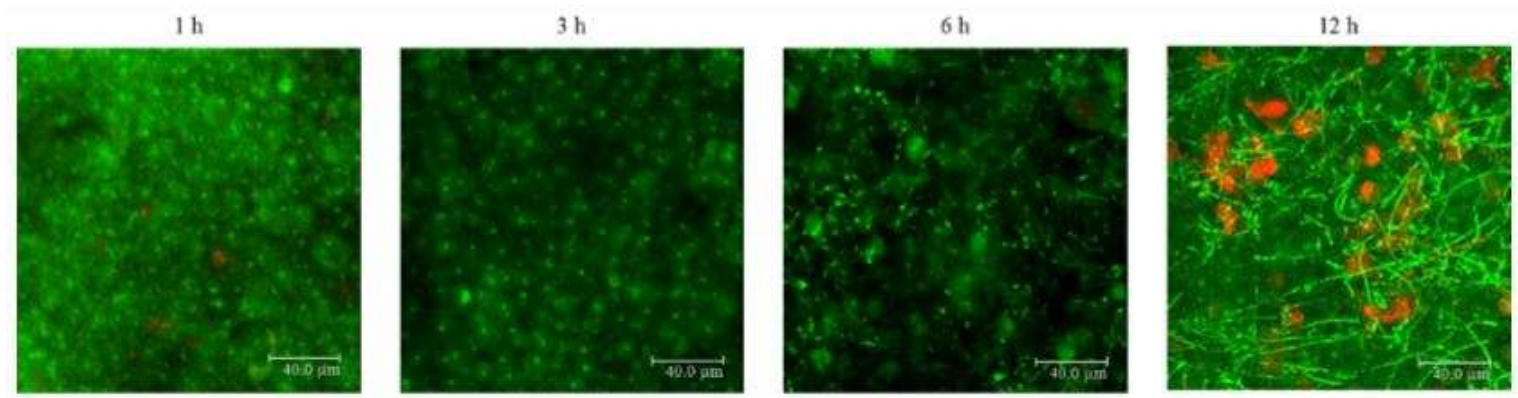
647 **Figure 2**



648

649

650 **Figure 3**



651

652

653

654

655

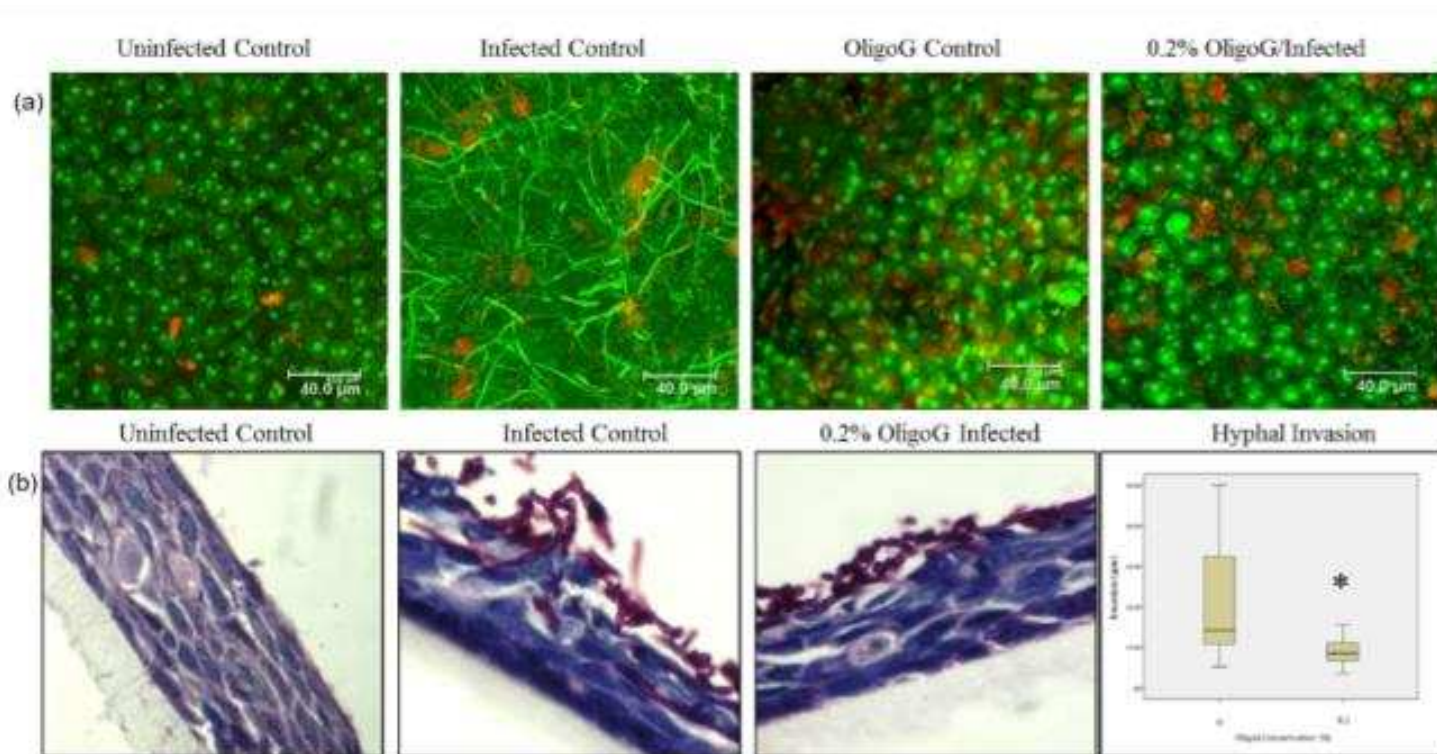
656

657

658

659 **Figure 4**

660



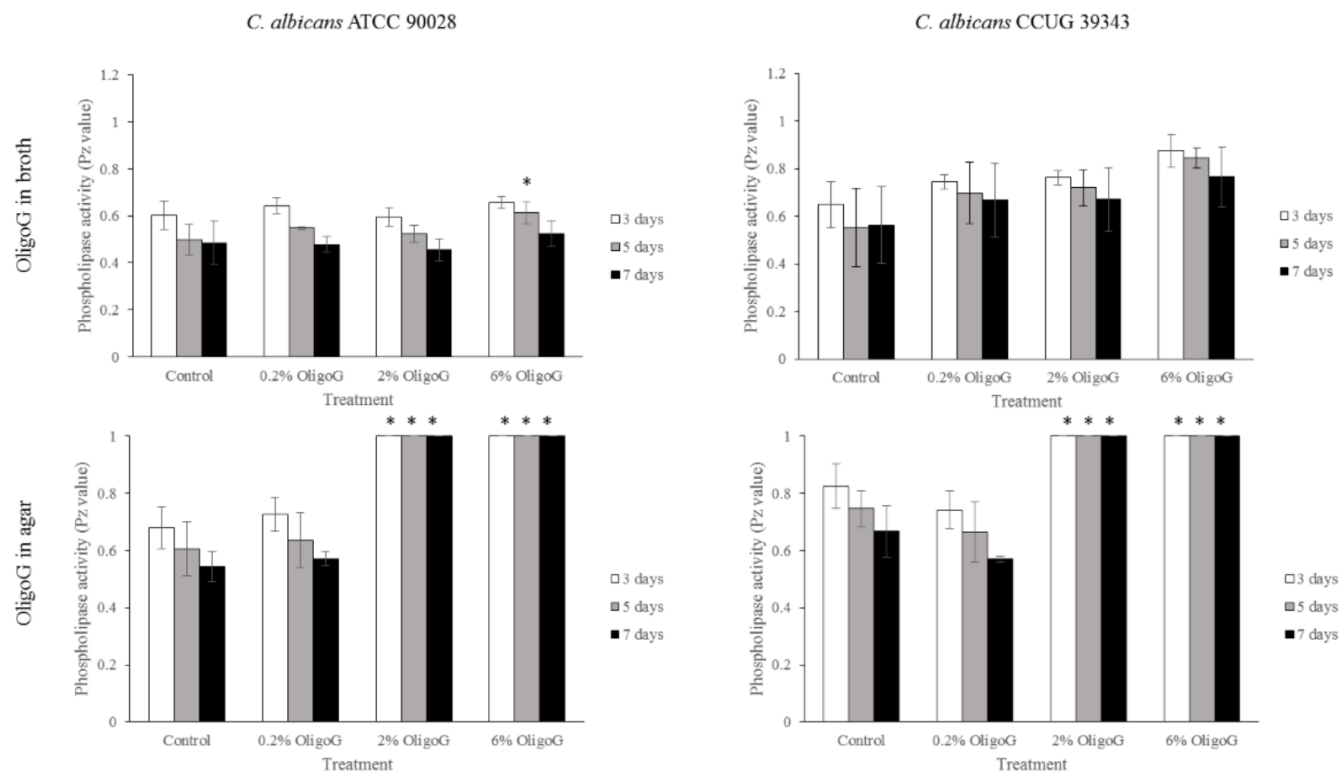
661

662

663

664 **Figure 5**

665

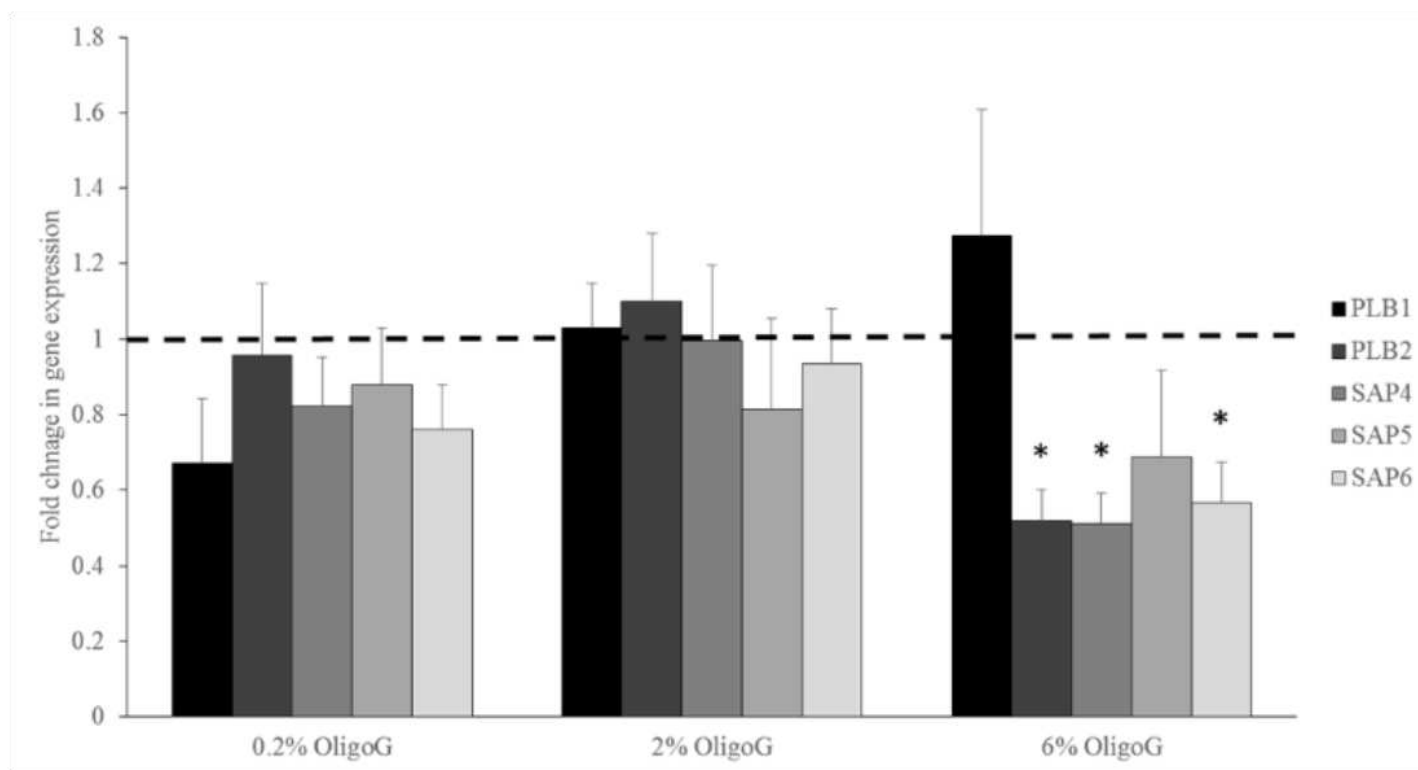


666

667

668

669 **Figure 6**



670

671